EUROFUSION WPMST1-CP(16) 15160

A Hakola et al.

Plasma-wall interaction studies in the full-W ASDEX Upgrade during helium plasma discharges

Preprint of Paper to be submitted for publication in
Proceedings of 26th IAEA Fusion Energy Conference

This work has been carried out within the framework of the EUROfusion Consortium and has received funding from the Euratom research and training programme 2014-2018 under grant agreement No 633053. The views and opinions expressed herein do not necessarily reflect those of the European Commission.

Plasma-wall interaction studies in the full-W ASDEX Upgrade during helium plasma discharges

A. Hakola[1], S. Brezinsek[2], D. Douai[3], M. Balden[4], V. Bobkov[4], D. Carralero[4], H. Greuner[4], A. Kallenbach[4], K. Krieger[4], G. Meisl[4], M. Oberkofler[4], V. Rohde[4], P. Schneider[4], T. Schwarz-Selinger[4], A. Lahtinen[5], G. De Temmerman[6], R. Caniello[7], F. Ghezzi[7], T. Wauters[8], A. Garcia-Carrasco[9], P. Petersson[9], I. Bogdanovic Radovic[10], Z. Siketic[10], ASDEX Upgrade Team, EUROfusion MST1[*]

[1]VTT Technical Research Centre of Finland, P.O.Box 1000, 02044 VTT, Finland
[2]Forschungszentrum Jülich GmbH, 52425 Jülich, Germany
[3]CEA, IRFM, 13108 St. Paul Lez Durance Cedex, France
[4]Max-Planck-Institut für Plasmaphysik, Boltzmannstrasse 2, 85748 Garching, Germany
[5]University of Helsinki, Department of Physics, P.O.Box 64, 00014 University of Helsinki, Finland
[6]ITER Organization, 13067 St. Paul Lez Durance Cedex, France
[7]Istituto di Fisica del Plasma - CNR, Via. Cozzi 53, 20125 Milan, Italy
[8]Laboratory for Plasma Physics, ERM/KMS, 1000 Brussels, Belgium, TEC Partner
[9]Department of Fusion Plasma Physics, Royal Institute of Technology, 10044 Stockholm, Sweden
[10] Rudjer Boskovic Institute, P.O.Box 180, 10002 Zagreb, Croatia
[*] See http://www.euro-fusionscipub.org/mst1
Email contact of main author: antti.hakola@vtt.fi

Abstract. Plasma-wall interaction was studied in the full-W ASDEX Upgrade during its dedicated helium campaign. Relatively clean plasmas with a He content of >80% could be obtained by applying ICWC discharges upon changeover from D to He. Surface analyses of W samples, however, indicated co-deposited layers with significant amounts of He and D being locally formed albeit globally D was released from the plasma-facing components. When exposing W samples to ELMy H-mode helium plasmas in the outer strike-point region of the divertor, no net erosion was observed but the surfaces had been covered with co-deposited layers. The layers were the thickest in the private flux region and extended throughout the OSP region in the case of rough and modified surfaces. Also, no clear signs of nanostructure growth or destruction could be seen The growth of such layers may impact the operation of future fusion reactors. Retention of He, for its part, remained small and uniform throughout the strike-point region.

1. Introduction

ITER has selected tungsten (W) to be used in the plasma-facing components (PFCs) of its divertor structures due to the good power-handling capabilities of W, low physical sputtering of W surfaces by plasma bombardment, and small retention of radioactive tritium (T) in the PFCs [1]. So far, the research activities have concentrated on the interaction of hydrogen (H) or deuterium (D) plasmas with W in linear plasma devices or in tokamaks such as JET [2] and ASDEX Upgrade (AUG) [3]. However, the possible start-up phase of ITER with helium (He) as well as alpha particles produced in D-T fusion reactions in its active phase have set the need to understand in detail the different plasma-wall interaction processes between He and W.

The most important research topics are quantifying the erosion, re-deposition, surface modification, and retention characteristics of W PFCs in different types of He plasmas. In addition, a smooth start of plasma operations in helium requires cleaning the vessel wall from residual fuel species of earlier discharges (e.g., H and D) as well as from various impurities (such as boron (B), carbon (C), nitrogen (N), and oxygen (O)) [4]. Compared to operations in H or D, the main difference in the response of W-based structures to He discharges will be the formation of nanoscale structures on them. Helium can induce bubbles in W, which will modify the surface in the nanoscale and, if the surface temperature as well as the fluence and energy of helium particles are high enough, a porous surface layer with coral-like tendrils, referred to as fuzz results. This has been observed experimentally in linear plasma devices [5,6]. Identifying the onset of fuzz formation in tokamaks

and temporal evolution of the modified surface layer during H-mode plasma operations are now a subject of joint experiments in different devices. Pioneering work has been carried out in TEXTOR [7] and Alcator C-Mod [8] - though so far only during L-mode or ELM-free H-mode operations.

We discuss the lessons learnt from two plasma-wall interaction experiments, carried out in AUG during its dedicated helium campaign in 2015. The results reported here have been obtained during standard H-mode AUG discharges in helium while the full scenario development took place only afterwards. Since then, advances have been made in developing ITER-relevant scenarios and efficiently controlling edge-localized modes (ELMs) using resonant magnetic perturbations under a large range of pedestal collisionality. Interestingly, fuelling efficiency is much higher in He than in D plasmas in AUG, resulting in lower divertor pressures at comparable pedestal pressures and hotter divertor plasmas, thus influencing PWI processes.

2. Start-up of helium plasma operations in AUG

When switching from H or D to He plasmas, the first wall need to be cleaned from fuel-containing co-deposited layers to guarantee good purity for the following experiments. Furthermore, after disruptions the vessel wall typically has to be conditioned to assist obtaining breakdown during subsequent plasma discharges. To this end, Ion Cyclotron Wall Conditioning (ICWC) is a good candidate, and it has already been tested in, e.g., JET, AUG, TEXTOR, and Tore Supra [4]. Here, we report the results obtained from a series of He-ICWC discharges before the 2015 helium campaign.

In ICWC, low-temperature (electron temperature T_e<10 eV) and low-density (electron density n_e=10^{16}-10^{18} m^{-3}) plasmas are formed resulting in a substantial flux of charge-exchange (CX) neutrals onto the wall structures [4]. Such particles can mobilize the fuel and impurity atoms residing in the material, resulting in removal rates up to 10^{17} D m^{-2} s^{-1} [4]. In the AUG experiment [9], two ion cyclotron resonance heating (ICRH) antennas were used during 20 discharges at 2.0 T, having a total duration of ~180 s. The power was 100-200 kW at 30 MHz. The fuel content of the vessel was monitored by the following means: (i) measuring the He content of the plasma during reference helium plasma discharges (electron density n_e = 9×10^{19} m^{-3}, plasma current I_p=0.8MA, toroidal magnetic field B_T=2.5T, auxiliary heating by neutral beam injection of 2.2MW, ICRH of 4.0 MW, and electron cyclotron resonance heating (ECRH) of 2 MW) before and after ICWC by the CX flux impinging on neutral particle analyzers (NPA), (ii) evaluating the temporal evolution of D_α (656.1 nm) and HeI (667.8 nm) spectral lines in the divertor and main-chamber regions, (iii) studying the composition of the exhaust gas using mass spectrometry, and (iv) measuring the changes in the D_2 and He contents of W samples exposed to plasmas in the outer midplane.

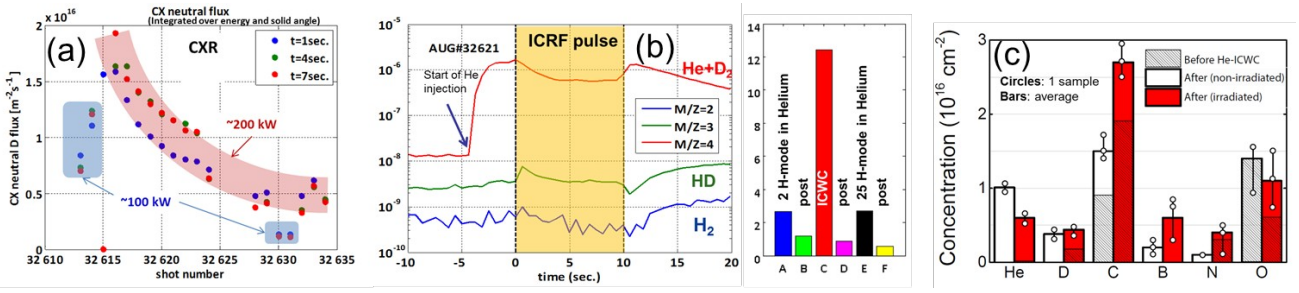

FIG 1. (a) NPA measurements for the release of D during the ICWC experiment. (b) Time traces for selected M/Z signals before, during, and after an ICWC pulse. The bar diagram has been extracted from outgassing measurements during a 170-hour long period. (c) Surface densities for selected elements on different W samples, exposed at the outer midplane, before and after the ICWC experiment.

Significant release of D from the wall structures could be observed during ICWC. This we notice from the CX data (FIG.1a), which show a peak in the beginning of the ICWC shots and gradual decrease towards the end of the experiment. Similar trend was observed by the spectroscopic measurements. The release rate was quantified on the basis of mass spectrometry. From the outgassing behaviour of the H_2, HD, and $He+D_2$ signals (FIG. 1b) a total amount of D being removed is ~13 Pa·m^3 per discharge, including 15 min of outgassing while during the reference plasma discharges only 3 Pa m^3 was measured. During overnight outgassing the amount remained <1 Pa m^3 ("post" in FIG. 1b). Simultaneously, the He content of the reference He pulses increased from He/(He+D+H)=0.4 before ICWC to 0.8 after the cleaning.

The efficiency of ICWC was estimated by surface analyses of bulk W samples before and after the cleaning phase (FIG. 1c) [10]. The samples were studied using Elastic Recoil Detection Analysis (ERDA) with a 10-MeV $^{28}Si^{3+}$ beam for the detection of He and D and using Time-of-Flight ERDA with a 36-MeV $^{127}I^{8+}$ beam to determine the concentrations of heavier impurities. Part of the samples had been pre-loaded with D in the PSI-2 plasma device but the initial D content turned out to be small, $<5\times10^{15}$ D cm^{-2}. As a result of ICWC, co-deposited layers containing D, B, C, N, and O were formed on all the samples with concentrations in the range $0.2\text{-}1.5\times10^{16}$ at cm^{-2} except for C. Boron originates from regular boronizations of the AUG vessel while the high C concentrations are due to the plasma loading in PSI-2 and from AUG PFCs with damaged W coatings on graphite substrates. The formation of such co-deposits may partly explain the apparent increase of the D content of all the samples during the experiment. One should, however, keep in mind that the analysed samples reflect a situation only at a particular location of the vessel, here the outer midplane. Although deuterium is globally removed from PFCs, it is then migrated in the scrape-off layer (SOL) plasma and ends up in shadowed areas at multiple erosion-deposition steps [11].

Interestingly, the helium concentration of the co-deposits was relatively high, up to 10^{16} He cm^{-2} (see FIG. 1c). This is comparable to the C or O contents of the surface layers, suggesting that He may substitute a substantial fraction of hydrogen atoms retaining on the samples and generally result in large fuel inventories on PFCs.

3. Erosion, deposition, and surface modifications of W PFCs at AUG

3.1 Samples and their characterization

The interaction of W PFCs with helium was investigated by exposing four poloidal rows of different samples to ELMy H-mode discharges in He at the outer strike-point (OSP) region of the AUG divertor [12]. The samples were mounted on two target tiles - two rows per target tile and 6 samples in each row - made of bulk W which were transferred to the desired location using the upgraded divertor manipulator (DIM-II) of AUG [13], see FIG. 2.

For each row, a different sample type was selected. On the first tile, bulk W samples were mounted at the centre, while W-coated (thickness 30 nm) graphite samples were positioned magnetically downstream of them. On the second target tile, the centre row consisted of W samples pre-damaged by He exposure in the high heat-flux device GLADIS [14] (denoted by T1-T6) while in the edge row bulk Mo samples had been positioned. The marker samples were used to determine erosion of W during the actual plasma experiment, the purpose of the Mo samples was to estimate re-deposition of W, while the two sets of W samples provided information on the changes in their surface morphology as well as formation or destruction of fuzz and retention of He on them.

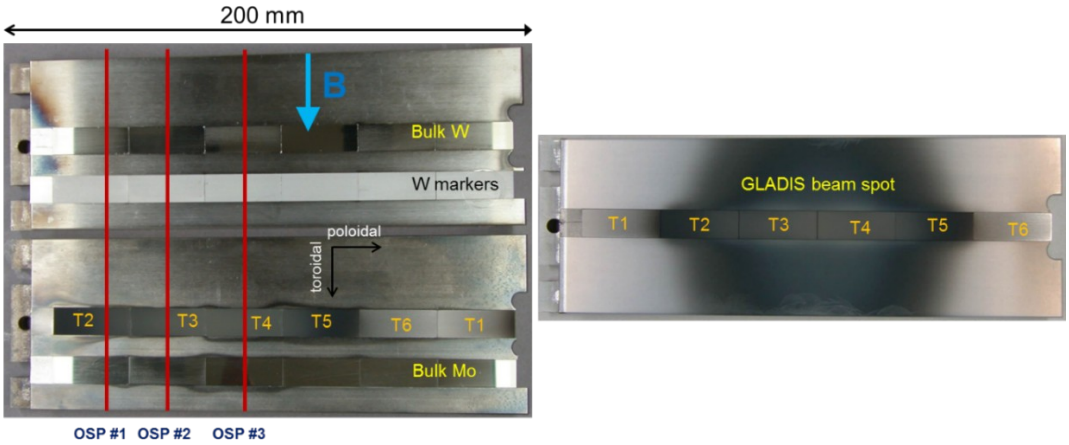

FIG. 2. (Left) Photograph of the 4 sample types mounted in the target tiles after the plasma experiment. The pre-damaged samples are labelled with symbols T1-T6 and the OSP positions for the three phases of the plasma experiment have been marked with red lines. Private flux region is located on the very left. (Right) Photograph of the pre-damaged probes T1-T6 after their exposure in GLADIS.

The pre-damaged samples contained a variety of nanostructures on the surfaces, ranging from small He bubbles to fully formed W fuzz with a layer thickness of ~2-3 μm. The nanostructures were produced by mounting bulk W samples on a target plate and exposing them to a pure He beam with an energy of 37 keV. A photograph of the sample surface after the GLADIS treatment is also visible in FIG. 2. At the centre of the holder, the surface temperature was ~2300 K and the He fluence around 1.0×10^{24} He^+ m^{-2}, while close to the edges the corresponding values were 1300 K and 0.4×10^{24} He^+ m^{-2}. Based on studies in linear plasma devices, tendril-like networks start to be formed as the surface temperature is T_s>1000 K, the energy of the incoming ions E_{in}>20 eV, and the fluence $\Phi>10^{24}$ He^+ m^{-2} [5,6]. Thus, the two samples at the centre show fully developed fuzz with coral-like features while in the peripheral zone only He nanobubbles in a W matrix are visible.

The most extensively modified samples were mounted closest to the OSP positions during the experiment while the samples with more benign surface modifications towards the upper edge of the target tile. The surface morphology of all the samples was investigated by scanning electron microscopy (SEM) and focused ion beam (FIB) studies. The erosion of the marker coatings was determined by Rutherford Backscattering Spectroscopy (RBS), using 2.0-MeV $^4He^+$ ions for the samples before and after the plasma experiment. After that all the samples were measured by Nuclear Reaction Analysis (NRA), where 3.8-MeV $^3He^+$ ions were applied to determine the deposition of different elements, primarily D, B, C, and N on the surfaces.

3.2 Plasma conditions during sample exposure

The W samples were exposed to plasma discharges in the lower single null (LSN) configuration with the following parameters: I_p=0.8 MA, B_t=2.5 T, auxiliary heating with ECRH of 2.6 MW at 140 GHz, NBI of 2.1 MW with equal share of H and He beams, and ICRH of 4.0 MW at 36.5 MHz. The average density was n_e=9-10×10^{19} m^{-3}. Altogether 25 identical shots were carried out such that the OSP position was varied between three poloidal locations (marked in FIG. 2) [12]. The overall exposure times for the three phases were ~100 s, ~60 s, and ~10 s, respectively. The D content of the plasma remained at a constant level of ~10% during the experiment and slowly decreased to <5% by the end of the He campaign. The H and He contents showed large fluctuations due to H beams used for plasma heating and, on average, the He content did not increase much from the starting value of 80% obtained by ICWC.

In the first part of the experiment (100 s), the OSP was poloidally set on the lowermost samples such that the pre-damaged sample T2, its surface being on the verge of nanostructure formation, could be exposed. This way one could investigate whether the nanofeatures were grown during the exposure. In the second phase, the OSP was moved upwards such that the sample T3 with a coral-like surface was subjected to the highest particle and power fluxes. The main motivation was to investigate erosion of W nanostructures by ELMs as well as further modifications of the surfaces. In phase I, only type III ELMs in the kHz regime were produced while in phase II, type I ELMs at 120-Hz frequency were observed, resulting from reduced fuelling between the two phases. In the third phase, the OSP was further raised and N_2 was injected to study the impact of N on the nanostructures; these results will be discussed elsewhere.

The energy and fluence were measured to be sufficient for inducing nanostructure formation and growth. Based on Langmuir probe measurements in the vicinity of the OSP, the ion saturation current was 2-2.5×10^{23} $m^{-2}s^{-1}$ and T_e=20-25 eV. Assuming that the impinging ions are mostly He^+, we obtain for the impact energy E_{in} ~100-150 eV, well above the threshold of 20 eV. From the 80% He content of the plasma, the fluence during phases I and II of the experiment is 1-2×10^{25} He^+ m^{-2}, an order of magnitude more than the 10^{24} He^+ m^{-2} limit mentioned in section 3.1. The surface temperature of the samples could not be directly measured but infrared measurements from neighbouring standard wall tiles indicate T_s>800 K. The samples, however, were much hotter due to their poor thermal contact with the target tiles, thus values higher than 1000 K are expected.

3.3 Results and conclusions

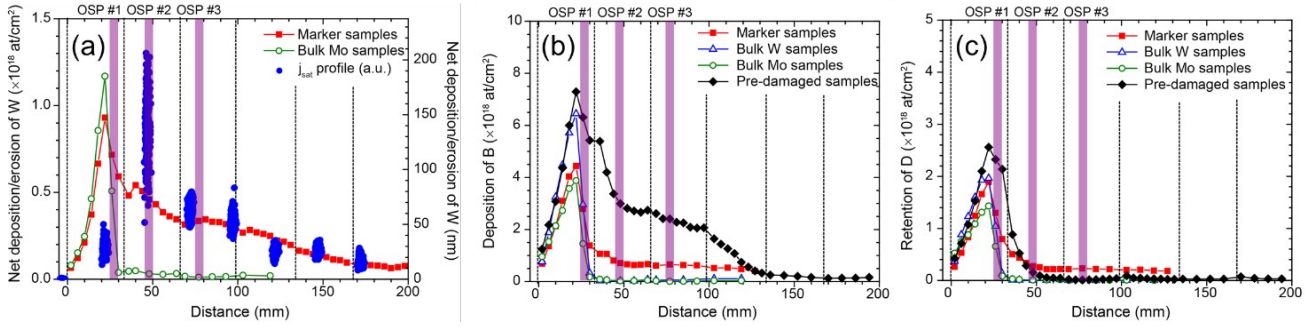

FIG. 3. (a) Poloidal net deposition/erosion (positive/negative values) profile for the W marker sample and re-deposition profile for W on the bulk Mo samples. Also the profile for the ion saturation current during phase II of the experiment is shown. (b) Poloidal deposition profile for B on the different samples. (c) Poloidal retention profile for D on the different samples. The purple bars denote the OSP positions during the three phases of the experiment.

The main observations can be summarized as follows:

- No net erosion was observed to take place in the experiment but the amount of W on the marker samples had increased by dozens of nm as a result of the plasma exposure (FIG. 3a). Thus, the entire OSP region is dominated by net deposition with the thickest layers in the private flux region (PFR), below all the OSPs of the experiment. This is in sharp contradiction with what has earlier been reported for D plasmas: a distinct net erosion peak at the strike point and net deposition regions surrounding it [15]. FIG. 3, in contrast, suggests that in helium plasmas a strong influx of material is established from the main chamber to the divertor, where it is further transported along the magnetic field lines and poloidally by the **E**×**B** drift towards the PFR [16].
- All the samples are covered with thick co-deposited layers consisting mainly of D, B, C, N, O, and W. The deposition profiles are qualitatively similar to the net deposition profiles for

W in FIG. 3a, as shown in FIGS. 3b and 3c for B and D. Again the most dominant peak is observed in the PFR.

- The rougher the sample surface, the more material is deposited on it, particularly above the OSP. The strongest deposition is measured on the pre-damaged samples with a large effective surface area while on the smooth bulk W and Mo samples deposition outside the PFR is almost non-existent. This is in line with the conclusions made in [17,18] on rough surfaces favouring accumulation of material in shadowed valleys behind protruding surface peaks.
- For tungsten, however, the deposition peak in the PFR is almost independent of the surface roughness but relatively rough marker samples and smooth bulk Mo samples indicate net deposition being comparable (FIG. 3a). This can be interpreted such that below the strike point the cold plasma conditions favour layer-by-layer growth of material and the memory of the original surface is lost. On the other hand, on the pre-damaged and bulk W samples much more impurities in the PFR than on the two other samples have been measured but this could be simply due to their different toroidal positions, as one can notice in FIG. 2.
- No signs of nanostructure erosion or formation is observed on the pre-damaged samples, nor on the bulk W samples. This is attributed to the deposited layer being quickly formed on the surface and covering all the nanostructures, thus protecting them from further exposure as FIB images in FIG. 4 illustrate. Around the OSP, a few individual corals had been eroded by ELMs before the entire surface had been covered with a deposited layer (FIG. 4a) while deeper in the PFR the co-deposit can be seen to consist of >20 sublayers (FIG. 4b).

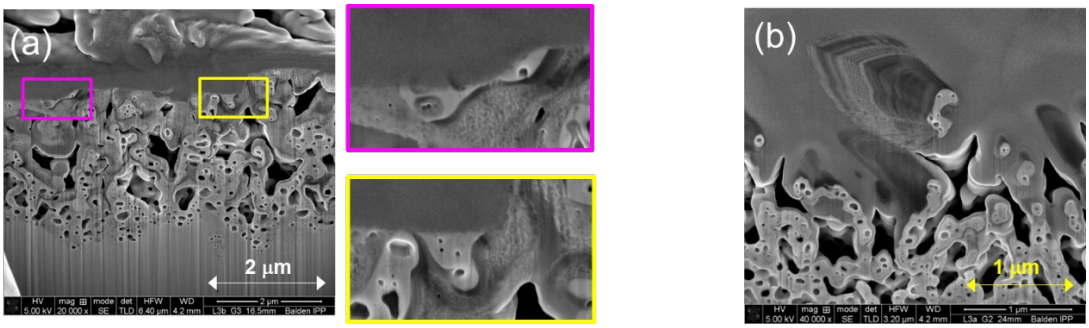

FIG. 4. (a) FIB images of the sample T3 close to the OSP. The two zoom-ins of the interface between the original nanostructure and the deposited layer have been marked with purple and yellow rectangles. (b) FIB image of the sample T2 in the PFR. The layered structure of the co-deposit is clearly visible.

We conclude that erosion of W surfaces and nanostructure formation or growth is overcompensated by local deposition of material in between ELMs, possibly resulting from erosion in the main chamber. The situation is quite unlike the case during D operations when large net erosion is typically measured around the strike point [15]. Different main-chamber sources are indeed plausible explanations to the apparent discrepancies: in the experiment discussed above, ICRH-heated plasmas were applied leading to strong sputtering of material from the limiter structures surrounding the ICRH antennas [19]. The process is further amplified by fast ions and heavy projectiles impinging on the PFCs in the main chamber.

4. Retention of helium in tungsten samples

The He content of selected samples was measured using foil-ERDA with 15-MeV $^{16}O^{5+}$ ions and time-of-flight ERDA with 23-MeV $^{127}I^{6+}$ ions. In both cases, only the topmost surface layer (50-100 nm) could be analysed, but based on earlier studies, under low-energy and low-flux irradiations, as is the case in the AUG experiment, He is typically retained close to the surface due to high probability of trapping in defects [20].

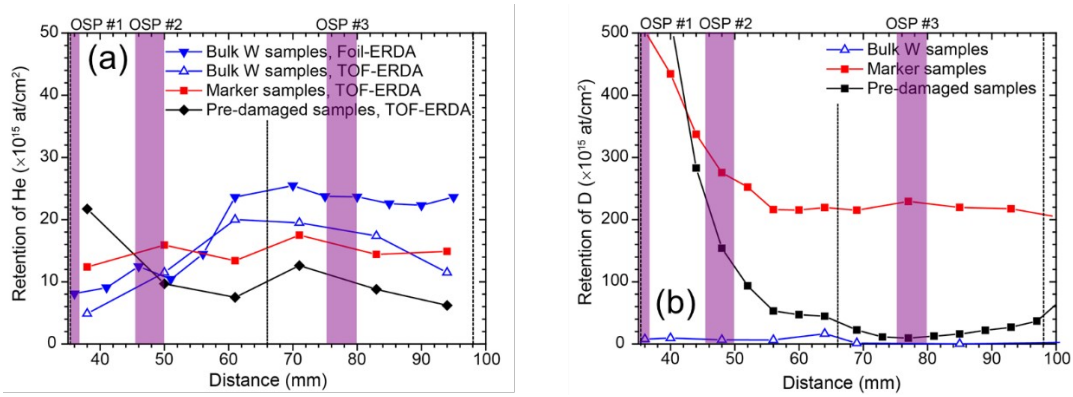

FIG. 5. (a) Poloidal retention profile for He on the different samples around the OSP region. (b) Poloidal retention profile for D on the different samples around the OSP region (zoom in of the data in FIG. 3c). The purple bars denote the OSP positions during the three phases of the experiment.

The different ERDA profiles are shown in FIG. 5a for the analysed samples, located in the vicinity of the OSP, on the SOL side of it. On the W samples, the He content is ~1-3×10^{16} He cm^{-2}, which is of the same order of magnitude as the surface densities measured on the W samples after the ICWC experiment (see section 2). The profile is also relatively flat with some point-to-point oscillations but no major increase in retention towards the PFR, as was, e.g., the case for D (see FIG. 5b where the data of FIG. 3c is reproduced at a higher magnification). This indicates that He stays in the vicinity of the surface, either trapped in defects and pores or the topmost layer of the growing co-deposit, as proposed in [20,21]. Our results also support the idea of saturation such that the surface densities would remain <10^{17} He cm^{-2} [22].

For the pre-damaged samples, the He content is comparable to that of bulk W samples or slightly lower. This would indicate retention being independent of the substrate and its roughness, although the results have to treated with caution since also the original nanostructured surface contained lots of He from the GLADIS exposure. Finally, the milled marker samples behaved similarly to the bulk W samples in terms of fuel retention. Here, of course, roughness is an issue since the analysis of ERDA results assumes the surface to be completely flat.

5. Conclusions

In this article we have studied plasma-wall interaction effects in the full-W ASDEX Upgrade during its dedicated helium campaign in 2015. Relatively clean plasmas with a He content of >80% could be obtained by applying ICWC discharges upon changeover from D to He. The D content of the plasma then slowly decreased during the entire He campaign while the He concentration did not change much due to continuous heating of the plasmas with hydrogen NBIs. Surface analyses of W samples, however, indicated co-deposited layers being formed on them which contained, besides He, significant amounts of D. This can be explained by multiple erosion-deposition steps albeit globally D was released from the PFCs.

When exposing different W samples to ELMy H-mode helium plasmas in the outer strike-point region of the divertor, no net erosion was observed but the sample surfaces had been covered with co-deposited layers. The layers were the thickest in the private flux region and extended throughout the OSP region in the case of rough and modified surfaces. Also, no clear signs of nanostructure growth or destruction could be seen. Since under D plasma operations the OSP co-incides with a region of measurable net erosion, we conclude that in He plasmas extra W sources, presumably in the main chamber, result in efficient coverage of the W surfaces during the first couple of seconds.

The growth of such layers may impact the operation of future fusion reactors even though retention of He on the surfaces seem not to be so much dependent on the substrate and its roughness. Instead, retention profiles are relatively homogeneous throughout the OSP region. Nevertheless, dedicated lab experiments and modelling efforts in the presence of impurity mixes are needed to enlighten the issue further and determine its significance for the operation of ITER.

Acknowledgements

This work has been carried out within the framework of the EUROfusion Consortium and has received funding from the Euratom research and training programme 2014-2018 under grant agreement No 633053. The views and opinions expressed herein do not necessarily reflect those of the European Commission.

References

[1] PHILIPPS V., J. Nucl. Mater. **415** (2011) S2.
[2] BREZINSEK S. *et al.*, J. Nucl. Mater. **463** (2015) 11.
[3] NEU R. *et al.*, J. Nucl. Mater. **438** (2013) S34.
[4] DOUAI D. *et al.*, J. Nucl. Mater. **463** (2015) 150.
[5] BALDWIN M. J. *et al.*, Nucl. Fusion. **48** (2008) 035001.
[6] KAJITA S. *et al.*, Nucl. Fusion **49** (2009) 095005.
[7] UEDA Y. *et al.*, J. Nucl. Mater. **415** (2011) S92.
[8] WRIGHT G.M. *et al.*, Nuclear Fusion **52** (2012) 042003.
[9] DOUAI D. *et al.*, "Changeover from Deuterium to Helium with Ion Cyclotron Wall Conditioning and diverted plasmas in ASDEX Upgrade, 22nd PSI Conference", Rome, Italy, 2016.
[10] GARCIA-CARRASCO A. *et al.*, "Investigation of probe surfaces after ion cyclotron wall conditioning in ASDEX Upgrade", 22nd PSI Conference", Rome, Italy, 2016.
[11] STRACHAN J. D. *et al*., Nucl. Fusion **48** (2008) 105002.
[12] BREZINSEK S. *et al.*, "Erosion of He pre-exposed tungsten samples by He plasmas in the divertor manipulator of ASDEX Upgrade", 22nd PSI Conference, Rome, Italy, 2016.
[13] HERRMANN A. *et al*., Fus. Eng. Des. **98-99** (2015) 1496.
[14] GREUNER H. *et al.*, J. Nucl. Mater. **417** (2011) 495.
[15] HAKOLA A. *et al.*, Physica Scripta **T167** (2016) 014026.
[16] HAKOLA A. *et al.*, "ERO and PIC simulations of gross and net erosion of tungsten in the outer strike-point region of ASDEX Upgrade", 22nd PSI Conference, Rome, Italy, 2016.
[17] SCHMID K. *et al.*, J. Nucl. Mater. **463** (2015) 66.
[18] HAKOLA A. *et al.*, Phys. Scr. **T159** (2014) 014027.
[19] BOBKOV V. *et al.*, Nucl. Fusion **53** (2013) 093018.
[20] TOKUNAGA K. *et al.*, J. Nucl. Mater. **313-316** (2003) 92.
[21] HU C. *et al.*, Fus. Eng. Des. **112** (2016) 117.
[22] HINO T. *et al.*, J. Nucl. Mater. **266-269** (1999) 538.